The influence of a building on the ground-borne vibration from railways in its vicinity

Xiangyu Qu[1], David Thompson[1], Evangelos Ntotsios[1] and Giacomo Squicciarini[1]

[1] Institute of Sound and Vibration Research, University of Southampton, Southampton SO17 1BJ, United Kingdom
Xiangyu.Qu@soton.ac.uk

Abstract. A finite element numerical model and a semi-analytical model are used to analyse the influence of buildings on ground vibration from underground railways. The insertion loss of a building with four types of foundations is examined using a 3D finite element model. Additionally, a semi-analytical model is built to analyse the vibration of the ground with the influence of a building with a pile foundation. This model is divided into two parts: a finite element model that represents the building as a column-shell structure and a semi-analytical model that simulates the infinite free-field ground. The foundations can amplify or attenuate the ground vibration in different frequency regions. For an example case, both models give similar insertion loss results due to a building in the transmission path, although there are differences due to the modelling assumptions. The findings suggest that when predicting the ground surface response induced by an underground railway, the surrounding buildings should be included in the calculations to get more accurate results.

Keywords: railways, ground vibration, finite element model, semi-analytical model, soil-structure interaction.

1 Introduction

Train-induced ground vibration from underground railways can cause disturbance to local residents through feelable vibration or ground-borne noise [1]. Many numerical [2, 3] and semi-analytical models [4] have been developed to study the problem. To obtain calculation results conveniently and quickly, it is usual to predict the vibration of the ground in free-field conditions, and to combine this with building transfer functions. This means that the impact of the presence of other building foundations between the vibration source (track) and the receiver position is neglected. In reality, between the track and the target buildings (i.e., the buildings for which predictions are made), or around the target buildings, there may be many other buildings. The presence of these buildings can have an impact on the ground vibration. Therefore, to improve the accuracy of ground vibration predictions, the influence of these surrounding buildings should be investigated.

A variety of technical methods are used to analyse the role of soil-building interaction. In [5] the effects of piled and raft foundations on the vibration level transmitted

into structures near railway tunnels are evaluated using a simple analytical model. The sub-modelling technique [6] has been developed based on a dynamic stiffness matrix of the soil coupled to the receptance matrix of the building. The soil-pile interaction was ensured at a series of coupled nodes between the soil and the piles. In [7] a subdomain formulation was used to predict the free-field vibration due to pile driving. In [8] the boundary element method is applied to investigate the effects of a group of buildings on ground vibration. Results from numerical simulations and measurements are presented in [9] in terms of the coupling loss, which is well-adapted for use with the empirical method. In [10] a simplified building-soil coupled model in the time domain is introduced by using simplified spring elements to represent the soil-structure interaction.

In this paper, two different models are used to investigate the impact of a building on the ground response in its vicinity. These are a 3D time domain finite element (FE) numerical model, and a semi-analytical frequency domain model. The effect of introducing the building is expressed as an insertion loss to evaluate the influence of the building on the ground vibration and the two models are compared.

2 Time-domain 3D numerical model

2.1 Model description

To compare the ground vibration with and without a structure, a 3D finite element model was created in ABAQUS, which consists of a tunnel in layered soil and a four-storey building. Infinite elements are placed at the boundaries of the model to suppress wave reflections. A separate model of a train passing over a section of track is used to generate a set of force time histories at the fastener locations which are then applied to the base of the tunnel in the FE model. A sketch of the two models is shown in Fig. 1. The fasteners and elastic supports are represented by spring and damper elements. The elastic supports are utilised to approximate the flexibility of the tunnel and soil. Both models operate in the time domain.

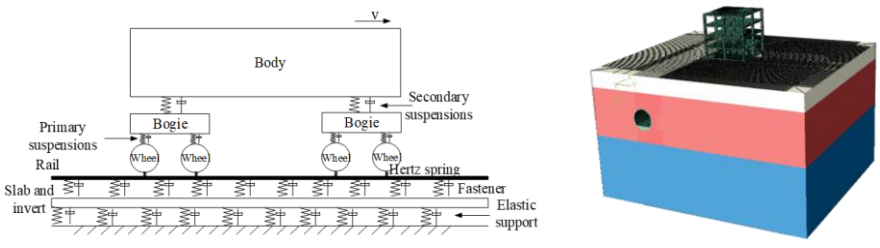

(a) (b)

Fig. 1. The numerical FE models with sub-models: (a) 2D train-track model used to generate fastener support forces and (b) 3D tunnel-soil-building model.

For the building, four different foundation types are evaluated (strip, raft, pile, and box), depicted in Fig. 2. The 8 m deep pile and 4.8 m deep box foundations are deep foundations, whereas the strip and raft foundations are shallow foundations, with depth 2.4 m.

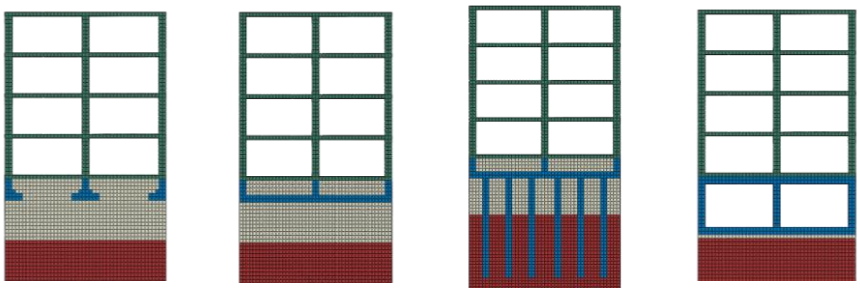

(a) (b) (c) (d)

Fig. 2. Different foundation types modelled in ABAQUS: (a) strip foundation; (b) raft foundation; (c) pile foundation and (d) box foundation.

Each span in the building is 6.6 m wide, the thickness of the wall is 0.6 m and the height of each storey is 3 m. The parameters of the materials in this model are listed in Table 1. The soil parameters are related to Beijing Metro line 5 [11]. Rayleigh damping is used for each material. The Rayleigh damping is proportional to a linear combination of mass and stiffness. The Rayleigh damping coefficient for mass, α=0.248, and the coefficient of stiffness $\beta=7.86\times10^{-5}$.

Table 1. The parameters used for each soil layer and the concrete [11]

Materials	Density (kg/m^3)	Young's modulus (N/m^2)	Poisson's ratio	Height (m)	Shear wave velocity (m/s)	Compressional wave velocity (m/s)
Layer 1	1850	1.31×10^8	0.344	5.0	162	333
Layer 2	2030	4.75×10^8	0.319	15.7	298	578
Layer 3	2150	6.98×10^8	0.268	33.0	358	636
Concrete	2500	3.60×10^{10}	0.28	-	-	-

2.2 Results

To assess the impact of different buildings and foundations, the vibration of the ground surface is shown in the form of an insertion loss (IL) relative to the free-field case. This is determined at a grid of 640 receiver points, shown in Fig. 3(a), which is used to produce contour plots of the IL. In addition, the IL is plotted at 8 points located along a line passing through the centre of the building. These receiver points are shown in Fig. 3(b); e.g., N25 denotes a point at a distance of 25 m from the tunnel centreline.

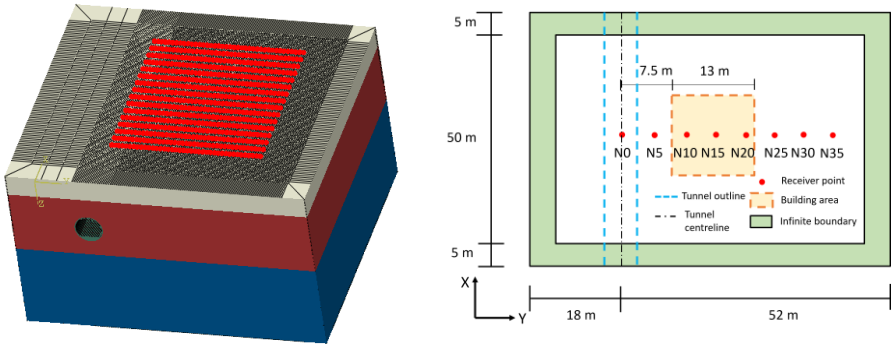

(a) (b)

Fig. 3. The receiver points at the ground surface: (a) receiver points used to plot contours and (b) line of receiver points.

Insertion loss results in the 50 Hz one-third octave band are shown in Fig. 4. This indicates that there can be areas of attenuation or amplification behind the structure. In Fig. 4(a), which shows results for the piled foundation, there are several zones of high positive IL close to the building column locations, indicating that vibration has been reduced by the presence of the structure and foundation. However, behind and in front of the building there are zones in which the vibration is increased (behind the building this was initially an area of low vibration amplitude). Fig. 4(b) compares the four foundation types at 50 Hz. At this frequency the IL is largest at locations directly beneath the structure. The IL is larger for the deep foundations than for the shallow foundations. However, the vibration behind the structure is increased more by the shallow foundations than by the deep foundations.

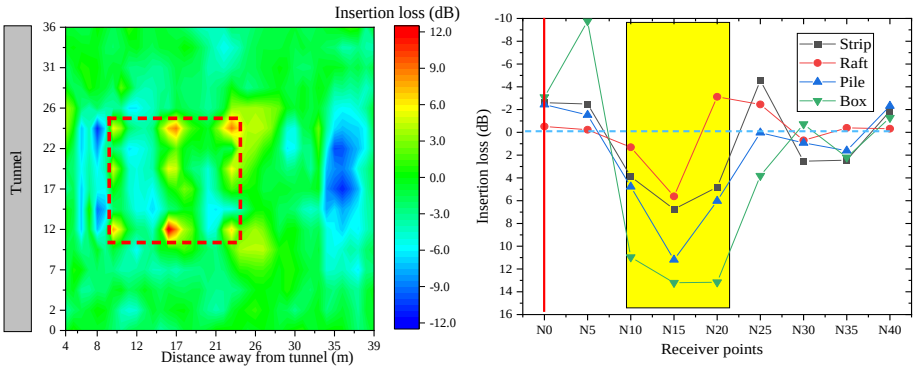

(a) (b)

Fig. 4. The insertion loss at 50 Hz: (a) contour of IL in dB for pile foundation (building location in red) and (b) IL on centreline of building (building location in yellow zone and tunnel position marked in red line).

The IL spectra for the four different foundations at N15 (beneath the building) and N30 (behind the building) are shown in Fig. 5. At the receiver point N15, at low frequencies, the insertion loss is close to zero. The vibration is attenuated in the regions 6.3-16 Hz and 32-80 Hz (the IL value is positive). Deep foundations have a greater impact on the vibration than shallow foundations. The IL values at N30 vary in a smaller range than those at N15. There is amplification in the region 10-16 Hz for all cases. Apart from the box foundation, all foundations have a vibration mitigation effect on the ground at this position behind the building at 40-50 Hz.

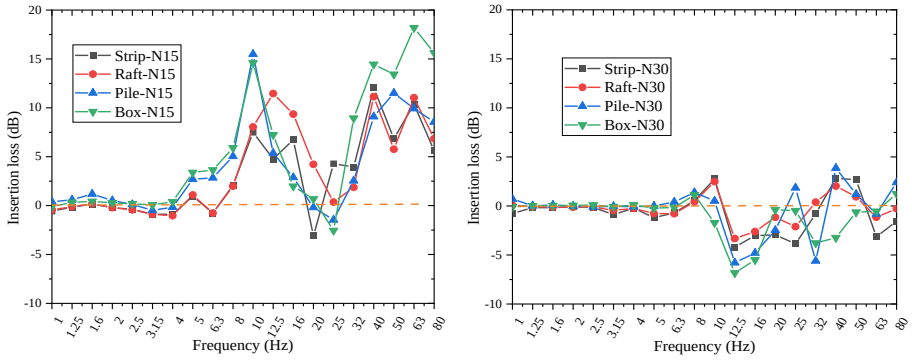

Fig. 5. Insertion loss spectra of four different foundation types at positions (a) N15 and (b) N30

3 Frequency domain semi-analytical model

3.1 Methodology

To create a model that can be used for parametric study, a semi-analytical train-track-tunnel model is coupled with a ground vibration model based on a frequency-wave-number domain dynamic stiffness matrix (DSM) method, using the method of [12, 13]. This is connected to a simple finite element building model, created using the Stabil Matlab toolbox [14]. The coupling method uses the sub-modelling approach in the frequency domain described in [5, 6]. The modelling approach is shown schematically in Fig. 6.

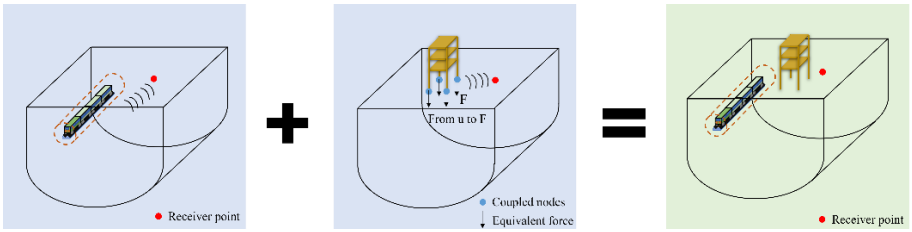

Fig. 6. Semi-analytical model sketch.

As shown in Fig. 6, the overall displacement at a receiver point (x_0, y_0, z_0) generated by the underground railway may be separated into two parts: the ground response caused by the train loads transmitted through the free field, $\hat{u}_0(x_0, y_0, z_0, \omega)$, and the response caused by the equivalent forces at the coupled nodes of the building. It can be written as

$$\begin{aligned}\hat{u}\left(x_0, y_0, z_0, \omega\right) = &\sum_{k=1}^{n} \hat{H}^G\left(x_{c,k} - x_0, y_{c,k} - y_0, z_{c,k} - z_0, \omega\right)\hat{F}\left(x_{c,k}, y_{c,k}, z_{c,k}, \omega\right) \\ &+\hat{u}_0\left(x_0, y_0, z_0, \omega\right)\end{aligned} \tag{1}$$

where $\hat{H}^G$ denotes the Green's function of the soil, and $\hat{F}(x_{c,k}, y_{c,k}, z_{c,k}, \omega)$ is the equivalent reaction force at coupled node *k*, with Cartesian coordinates ($x_{c,k}$, $y_{c,k}$, $z_{c,k}$).

As it is assumed that the displacement of the soil is equal to the displacement of the foundation at the coupled nodes, the displacement of the coupled nodes is obtained as

$$\begin{aligned}\hat{\mathbf{U}}_{\mathrm{g}}(\omega) &= \left(\mathbf{I} + \hat{\mathbf{H}}^{\mathrm{G}}\left(\omega\right)\hat{\mathbf{K}}'_{\mathrm{b}}\left(\omega\right)\right)^{-1}\hat{\mathbf{U}}_{\mathrm{s0}}\left(\omega\right) \\ &= \left(\mathbf{I} + \hat{\mathbf{H}}^{\mathrm{G}}\left(\omega\right)\left(\hat{\mathbf{K}}_{\mathrm{gg}}\left(\omega\right) - \hat{\mathbf{K}}_{\mathrm{gi}}\left(\omega\right)\hat{\mathbf{K}}_{\mathrm{ii}}\left(\omega\right)^{-1}\hat{\mathbf{K}}_{\mathrm{ig}}\left(\omega\right)\right)\right)^{-1}\hat{\mathbf{U}}_{\mathrm{s0}}\left(\omega\right)\end{aligned} \tag{2}$$

where $\hat{\mathbf{K}}'_{\mathrm{b}}(\omega)$ is the reduced dynamic stiffness matrix of the building model. It can be obtained from the full matrix by partitioning it into four sub-matrices $\hat{\mathbf{K}}_{\mathrm{ii}}$, $\hat{\mathbf{K}}_{\mathrm{ig}}$, $\hat{\mathbf{K}}_{\mathrm{gi}}$ and $\hat{\mathbf{K}}_{\mathrm{gg}}$, where the subscript i indicates the internal nodes of the building, and g indicates nodes of the building coupled to the ground. $\hat{\mathbf{U}}_{\mathrm{s0}}(\omega)$=$\hat{u}_0(x_{c,k}, y_{c,k}, z_{c,k}, \omega)$, the displacement at the coupled node positions induced by the train load in the tunnel without any building in the transmission path. $\hat{\mathbf{H}}^{\mathrm{G}}(\omega)$ is the soil transfer receptance matrix for the coupled node positions, which can be denoted as

$$\hat{\mathbf{H}}^{\mathrm{G}}\left(\omega\right) = \begin{bmatrix} \hat{\mathbf{H}}_{11}\left(\omega\right) & \hat{\mathbf{H}}_{12}\left(\omega\right) & \cdots & \hat{\mathbf{H}}_{1k}\left(\omega\right) \\ \hat{\mathbf{H}}_{21}\left(\omega\right) & \hat{\mathbf{H}}_{22}\left(\omega\right) & \cdots & \hat{\mathbf{H}}_{2k}\left(\omega\right) \\ \vdots & \vdots & \ddots & \vdots \\ \hat{\mathbf{H}}_{l1}\left(\omega\right) & \hat{\mathbf{H}}_{l2}\left(\omega\right) & \cdots & \hat{\mathbf{H}}_{lk}\left(\omega\right) \end{bmatrix} \tag{3}$$

where $\hat{\mathbf{H}}_{lk}(\omega)$ indicates the displacement at coupled node *l* due to a unit force at coupled node *k*. It can be calculated from the Green's function of the soil.

After the displacements of the coupling points are calculated, the equivalent forces acting at the coupled nodes are calculated using

$$\hat{\mathbf{F}}_{\mathrm{g}}(\omega) = \hat{\mathbf{K}}'_{\mathrm{b}}(\omega)\hat{\mathbf{U}}_{\mathrm{g}}(\omega) = \left(\hat{\mathbf{K}}_{\mathrm{gg}}(\omega) - \hat{\mathbf{K}}_{\mathrm{gi}}(\omega)\hat{\mathbf{K}}_{\mathrm{ii}}(\omega)^{-1}\hat{\mathbf{K}}_{\mathrm{ig}}(\omega)\right)\hat{\mathbf{U}}_{\mathrm{g}}(\omega) \tag{4}$$

In summary, the displacement response of the ground receiver point can be calculated as the sum of the components due to the train excitation and due to the reactions at the building.

3.2 Results and comparison

For simplicity, it is assumed that the piles are located directly beneath the building columns. To allow comparison, a similar arrangement is used in both the time-domain FE model and the frequency-domain semi-analytical model. Moreover, in this section, the soil is represented by a homogeneous half space instead of the layered soil used previously. The main dimensions of the model, including the location of the selected receiver point, are shown in Fig. 7(a). The insertion loss at this point calculated from these two models is shown in Fig. 7(b). The overall shape of the IL is similar in both results, although there are differences in the numerical values. Due to differences in the modelling assumptions, it is unavoidable that there are differences in some frequency bands.

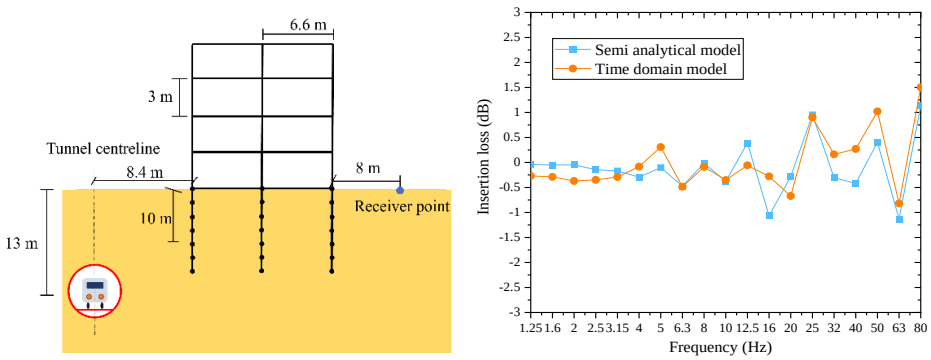

(a) (b)

Fig. 7. (a) Position of source and receiver point and (b) comparison between IL of the two models.

The semi-analytical model can estimate the effect of buildings on the vibration of the ground surface in the frequency domain and provide calculation results faster than the FE model. It can provide a suitable method for further investigation into the impact of the building and the source separately. However, this modelling approach is less flexible than the FE approach in terms of the foundation shapes it can consider. If there are too many coupled nodes, it will affect the calculation efficiency.

4 Conclusions

The presence of buildings between the railway and the target receiver point will influence the train-induced ground vibration. Results from numerical and semi-analytical models are presented to assess this effect. The numerical model can consider more details, which means different kinds of foundation shape can be considered. The semi-analytical model can calculate the influence of the buildings quickly and efficiently but

is less flexible. For an example case, both models give similar insertion loss results due to a building in the transmission path, although there are differences due to the modelling assumptions. The foundations can amplify or attenuate the ground vibration in different frequency regions. When predicting the ground surface response due to underground railways, the effects of neighbouring buildings should be included in the calculations to get more accurate results. Further investigation using this semi-analytical model can show the impact of the building and the source separately.

References

1. Thompson, D., Kouroussis, G., Ntotsios, E.: Modelling, simulation and evaluation of ground vibration caused by rail vehicles. Vehicle System Dynamics 57(7), 936-983 (2019).
2. Kouroussis, G., Connolly, D., Alexandrou, G., Vogiatzis, K.: Railway ground vibrations induced by wheel and rail singular defects. Vehicle System Dynamics 53(10), 1500-1519 (2015).
3. Yang, J., Zhu, S., Zhai, W., Kouroussis, G., Wang, Y., Wang, K., Lan, K., Xu, F.: Prediction and mitigation of train-induced vibrations of large-scale building constructed on subway tunnel. Science of The Total Environment 668, 485-499 (2019).
4. Xia, H., Cao, Y., De Roeck, G.: Theoretical modeling and characteristic analysis of moving-train induced ground vibrations. Journal of Sound and Vibration. 329(7), 819-832 (2010).
5. Kuo, K., Jones, S., Hunt, H., Hussein, M.: Applications of PiP: Vibration of embedded foundations near a railway tunnel. In: 7th European Conference on Structural Dynamics (EURODYN) pp. 7-9 (2008).
6. Hussein, M., Hunt, H., Kuo, K., Costa, P.: The use of sub-modelling technique to calculate vibration in buildings from underground railways. Proceedings of the Institution of Mechanical Engineers, Part F: Journal of Rail and Rapid Transit 229(3), 303-314 (2013).
7. Masoumi, H., Degrande, G.: Numerical modeling of free field vibrations due to pile driving using a dynamic soil-structure interaction formulation. Journal of Computational and Applied Mathematics 215(2), 503-511 (2008).
8. Coulier, P., François, S., Lombaert, G., Degrande, G.: Application of hierarchical matrices to boundary element methods for elastodynamics based on Green's functions for a horizontally layered halfspace. Engineering Analysis with Boundary Elements 37(12), 1745-1758 (2013).
9. Kuo, K., Papadopoulos, M., Lombaert, G., Degrande, G.: The coupling loss of a building subject to railway induced vibrations: Numerical modelling and experimental measurements. Journal of Sound and Vibration 442, 459-481 (2019).
10. López-Mendoza, D., Connolly, D., Romero, A., Kouroussis, G., Galvín, P.: A transfer function method to predict building vibration and its application to railway defects. Construction and Building Materials 232, 117217 (2020).
11. Xia, H.: Traffic induced environmental vibrations and controls: theory and application. Nova publication, New York (2013).
12. Hussein, M., François, S., Schevenels, M., Hunt, H., Talbot, J., Degrande, G.: The fictitious force method for efficient calculation of vibration from a tunnel embedded in a multi-layered half-space. Journal of Sound and Vibration 333, 6996-7018 (2014).
13. Ntotsios, E., Thompson, D., Hussein, M.: The effect of track load correlation on ground-borne vibration from railways. Journal of Sound and Vibration 402, 142-163 (2017).
14. François, S., Schevenels, M., Dooms, D., Jansen, M., Wambacq, J., Lombaert, G., Degrande, G., De Roeck, G.: Stabil: An educational Matlab toolbox for static and dynamic structural analysis. Computer Applications in Engineering Education 29(5), 1372-1389 (2021).